International Journal of Nanomedicine

Dovepress
open access to scientific and medical research

Open Access Full Text Article

ORIGINAL RESEARCH

Chitosan-Coated Selenium Nanoparticles Attenuate PRRSV Replication and ROS/JNK-Mediated Apoptosis in vitro

Chunyan Shao[1–5,*], Ziwei Yu[1–5,*], Tongwang Luo[1–5,*], Bin Zhou[1–5], Quanjiang Song[1–5], Zhuoyue Li[1–5], Xiaoqiang Yu[1–5], Sheng Jiang[1–5], Yingshan Zhou[1–5], Wanyu Dong[1–5], Xingdong Zhou[1–5], Xiaodu Wang[1–5], Houhui Song[1–5]

[1]Key Laboratory of Applied Technology on Green-Eco-Healthy Animal Husbandry of Zhejiang Province, Hangzhou, Zhejiang, 311300, People's Republic of China; [2]Zhejiang Provincial Engineering Research Center for Animal Health Diagnostics & Advanced Technology, Hangzhou, Zhejiang, 311300, People's Republic of China; [3]Zhejiang International Science and Technology Cooperation Base for Veterinary Medicine and Health Management, Hangzhou, Zhejiang, 311300, People's Republic of China; [4]China-Australia Joint Laboratory for Animal Health Big Data Analytics, Hangzhou, Zhejiang, 311300, People's Republic of China; [5]College of Animal Science and Technology & College of Veterinary Medicine, Zhejiang A&F University, Hangzhou, Zhejiang, 311300, People's Republic of China

*These authors contributed equally to this work

Correspondence: Houhui Song; Xiaodu Wang, College of Animal Science and Technology & College of Veterinary Medicine, Zhejiang A&F University, Hangzhou, Zhejiang, 311300, People's Republic of China, Tel +86 15064890670; +86 18806537583, Email songhh@zafu.edu.cn; xdwang@zafu.edu.cn

Introduction: Porcine reproductive and respiratory syndrome virus (PRRSV) is a highly prevalent and endemic swine pathogen that causes significant economic losses to the global swine industry. Selenium nanoparticles (SeNPs) have attracted increasing attention in the biomedical field, given their antiviral effects. This study aimed to investigate the inhibitory effect of chitosan-coated SeNPs (CS-SeNPs) on PRRSV replication.

Methods: In this study, CS-SeNPs were synthesized by chemical reduction and characterized by assessing the morphology, size distribution, zeta potential, and element composition. Marc-145 cells were infected with r-PRRSV-EGFP (0.1 MOI) and inoculated with CS-SeNPs (10 μM). Subsequently, the concentrations of hydrogen peroxide (H_2O_2) and glutathione (GSH), and glutathione peroxidase (GSH-Px) activity were measured using specific commercial assay kits. ORF5 RNA expression, viral titer, and nucleocapsid (N) protein expression were assessed using qRT-PCR, $TCID_{50}$, and Western blot. ROS generation, apoptosis rates, and JNK / caspase-3/PARP protein expression were evaluated using dihydroethidium staining, flow cytometry, and Western blot.

Results: The results showed that CS-SeNPs treatment significantly suppressed oxidative stress induced by r-PRRSV-EGFP infection by increasing GSH-Px activity, promoting GSH production, and inhibiting H_2O_2 synthesis. CS-SeNPs treatment significantly inhibited ORF5 gene expression, viral titers, and N protein of r-PRRSV-EGFP at 24 and 48 hours post-infection (hpi) in Marc-145 cells. The increase in apoptosis rates induced by r-PRRSV-EGFP infection was significantly decreased by CS-SeNPs inoculation through inhibiting ROS generation, JNK phosphorylation levels, and cleavage of caspase-3 and PARP mainly at 48 hpi.

Conclusion: These results demonstrated that CS-SeNPs suppress PRRSV-induced apoptosis in Marc-145 cells via the ROS/JNK signaling pathway, thereby inhibiting PRRSV replication, which suggested the potential antiviral activity of CS-SeNPs that deserves further investigation for clinical applications.

Keywords: chitosan-coated selenium nanoparticles, PRRSV, apoptosis, ROS, JNK signaling pathways

Introduction

Porcine reproductive and respiratory syndrome (PRRS), first reported in the United States in 1987, has become a pandemic responsible for huge economic losses each year worldwide.[1,2] The pathogenic agent is the PRRS virus (PRRSV), a positive-stranded RNA virus that belongs to the Arteriviridae family.[3] The clinical signs of PRRSV-infected sows are late-term abortion, premature delivery, fetal death, high pre-weaning mortality, and respiratory disease.[4] A key

Received: 13 April 2022
Accepted: 4 July 2022
Published: 7 July 2022

aspect of PRRSV virulence is that the virus can suppress the innate immune response and induce persistent infection.[5] In recent years, a novel PRRSV variant named NADC30-like, similar to the NADC30 strain in the United States in 2008, has become the dominant epidemic strain in numerous Chinese provinces.[6] The prevention and control of this disease are challenging since PRRSV has many strains and mutates quickly, with a complicated mechanism of virus infection and immune escape.[7,8] It has been shown that commercially available vaccines, including inactivated, live-attenuated and DNA vaccines, cannot provide adequate protection against PRRSV. Therefore, developing host-targeted antiviral drugs has become a new strategy for antiviral therapy.[9] The regulation of host-mediated apoptosis is one of the cellular mechanisms underlying PRRSV pathogenesis.[10] Moreover, it has been shown that changes in redox homeostasis during viral infection are linked to viral pathogenesis and oxidative stress induced by PRRSV in both cells and pigs.[11]

Selenium (Se) is a natural antioxidant essential for human and animal activities.[12] An increasing body of evidence suggests that multiple viral infections such as SARS-CoV-2, HIV-1, Coxsackie virus, and poliovirus are related to selenium deficiency.[13–16] Se nanoparticles (SeNPs) represent elemental Se particles at a nano-size scale with zero oxidation state (Se0) obtained through nanotechnology, possessing the advantages of low toxicity, degradability, and high bioavailability compared with organic and inorganic Se compounds.[17] In the past decade, SeNPs have attracted worldwide interest for therapeutic application in anticancer, antimicrobial, and antiviral activities.[18] Wang et al reported that SeNPs could inhibit H_1N_1 influenza virus-induced apoptosis by inhibiting ROS-mediated AKT and p53 signaling pathways.[19,20] Furthermore, as a drug carrier, SeNPs could enhance the antiviral effect of oseltamivir to suppress Enterovirus 71 (EV71) proliferation.[21] Moreover, simultaneous administration of Hepatitis B virus (HBV) antigen vaccine and SeNPs could promote lymphocyte proliferation and IFN-γ production.[22]

However, the mechanisms underlying the inhibitory effect of SeNPs on virus replication remain unclear. Hitherto, no research has assessed the effect of SeNPs on virus infection in swine. Chitosan (CS) is a kind of alkaline polysaccharide characterized by non-toxicity, good biocompatibility, biodegradability, and low immunogenicity.[23] Interestingly, the modification of SeNPs with CS (CS-SeNPs) can significantly improve the stability of SeNPs in an aqueous solution and antioxidant activity.[24] Accordingly, this study sought to investigate whether CS-SeNPs could affect PRRSV replication in vitro.

Materials and Methods

Cell Culture and Virus Infection

African green monkey kidney cell line Marc-145 purchased from ATCC were cultured in Dulbecco's Modified Eagle's Medium (DMEM; Gibco, Thermo Fisher Scientific) supplemented with 10% fetal bovine serum (FBS, Gibco) at 37°C in a humidified 5% CO_2 incubator. Marc-145 cells between passages 3 and 7 were used for the following experiments. rHP-PRRSV/SD16/TRS6-EGFP was a generous gift from Dr. Chengbao Wang (Northwest A&F University) and used for viral transfection. The recombinant PRRSV carrying an EGFP reporter gene as a separate transcription unit has widely been used for basic research on virus biology.[25] The virus was used to inoculate Marc-145 cells at a multiplicity of infection (MOI) of 0.1. The PRRSV ZJ/JX-2015 strain was isolated and stored in our lab.

Preparation of Chitosan-Coated Selenium Nanoparticles (CS-SeNPs)

CS-SeNPs were synthesized using chemical reduction as previously described by Zeng et al.[26] Briefly, 1.5 mL CS (10 mg/mL, Aladdin, China) was mixed with an equivalent volume of 0.1 M Na_2SeO_3 (Sigma, USA), then ultrapure water was added with a constant volume of up to 10 mL and stirred for 30 min. Subsequently, 1.5 mL of freshly prepared 0.4 M ascorbic acid (Solarbio, China) and 3.5 mL ultrapure water were added sequentially, then the mixed solution was sonicated at 14 kHz for 2 hours in darkness. The color of the solution changed from colorless to orange-red. The unreacted CS, Na_2SeO_3, and ascorbic acid were removed by dialysis (MWCO: 8000–12,000 Da) for 48 h at 4°C, and CS-SeNPs were obtained. The preparation process of SeNPs was the same as for CS-SeNPs, except that CS was replaced by an equal volume of ultrapure water.

Characterization of CS-SeNPs

For the morphological analysis of CS-SeNPs, a drop of nanoparticle solution was loaded on the carbon-coated copper grid for air-drying, then the samples were observed using transmission electron microscopy (JEM-1200EX, JEOL; Japan) at an accelerating voltage of 80 kV. The surface morphology of Se nanoparticles and elemental composition were studied under Raman Imaging and Scanning Electron Microscopes (RISE-Magna, TESCAN, Czech). The concentration of Se nanoparticles was determined by inductively coupled plasma mass spectrometry (i CAP Q ICP-MS, Thermo Scientific, USA). The size distribution and zeta potential of Se nanoparticles were measured by dynamic light scattering (DLS) using the Zetasizer Nano analyzer (Zetasizer NanoZS, Malvern Panalytical, Malvern, UK) as previously described by Awet et al.[27]

Measurement of Cell Viability

Cell viability was tested using a Cell Counting Kit-8 (CCK-8, Beyotime, Nanjing, China) according to the manufacturer's instructions. In brief, Marc-145 cells were inoculated into a 96-well plate at a density of 1×10^4 cells/well and cultured to 80% confluence. Then the cells were added with or without gradient dilution of CS-SeNPs at a final concentration of 0.1, 1, 10, 100 and 1000 μM and incubated at 37°C, 5% CO_2 for 48 h. After that, 10 μL CCK-8 solution was added to each well and incubated for another 2 h. Then, the optical density (OD) was measured at 450 nm using a Microplate Reader (BioTek Synergy H1, Agilent, USA), and the half-maximal inhibitory concentration (IC50) of CS-SeNPs was calculated using GraphPad Prism (version 7.0, GraphPad Software, San Diego, CA, USA).

Measurement of Hydrogen Peroxide (H_2O_2) and Glutathione (GSH) Concentration and Glutathione Peroxidase (GSH-Px) Activity

The concentrations of GSH and H_2O_2 and GSH-Px activity in the cell culture medium were measured using specific commercial assay kits (H_2O_2: A064; GSH: A006; GSH-Px: A005, Nanjing Jiancheng Bioengineering Institute, Nanjing, China) according to the manufacturer's instructions. The protein concentration in the cell lysate was measured using a BCA protein assay kit (Beyotime, China). H_2O_2 was reacted with molybdic acid to form a yellow complex, which was determined using a Microplate Reader (BioTek Synergy H1, Agilent, USA) at 405 nm. The level of H_2O_2 was expressed as mmol/g protein. The GSH level was estimated by the DTNB [5,5'- dithiobis (2-nitrobenzoic acid)] reduction method, and the absorbance was measured using a Microplate Reader (BioTek Synergy H1, Agilent, USA) at 420 nm. All samples were compared to a GSH standard curve and expressed as mg/g protein. The GSH-Px activity was measured at 412 nm by quantifying the rate of oxidation of reduced GSH to oxidized glutathione. All samples were tested in triplicates.

The Addition of CS-SeNPs and r-PRRSV-EGFP at Different Time Intervals

To evaluate the inhibitory effect of CS-SeNPs on PRRSV replication, a time-of-addition experiment was performed as shown in the timeline schematic, previously described by Liu et al.[28] Marc-145 cells were inoculated in 24-well plates and divided into 8 groups (control, I to VII) of 3 wells each. When the cells reached 80% confluence, 200 μL CS-SeNPs at a final concentration of 10 μM or an equivalent volume of H_2O was added and recorded as −1 h. At 0 h, the culture supernatants without CS-SeNPs were replaced in groups III and IV, CS-SeNPs were added to groups V and VI, then all group cells were inoculated with r-PRRSV-EGFP (0.1 MOI). At 1 h, the culture supernatants in all groups were discarded and replaced with (I, III, V and VII groups) or without (control, II, IV and VI groups) 10 μM CS-SeNPs. Incubation of all groups continued for 48 h; then, supernatants were harvested and used for total RNA extraction.

RNA Extraction and Absolute Real-Time Quantitative PCR

Total RNA was extracted from cell supernatants using TRIzol reagent (Thermo Scientific, USA), and first-strand complementary DNA (cDNA) was generated using a Reverse Transcription System Kit (TOYOBO, Japan) according to the manufacturer's instructions. Then, absolute quantitative mRNA levels of PRRSV ORF5 gene (5'-GAAATGCTTGACCGCGGGCT-3' and 5'- GTGTCAAGGAAATGGCTGGT −3') were calculated using its standard plasmid's amplification curve. In this regard, each RT-qPCR reaction was conducted using three replicates with a final

reaction volume of 20 μL per well, including 4 μL cDNA, 10 μL 2×SYBR Green Master mix (Vazyme, China), and 0.4 μL of upstream and downstream primers using an Mx3000P Real-Time PCR System (Agilent, USA).

Quantitative Assessment of Virus Titer

Viral titers in Marc-145 cells were determined for the median tissue culture infectious dose ($TCID_{50}$) as described previously.[29] Marc-145 cells were cultured in 96-well plates to reach 80% confluence and infected with 10-fold serial dilutions of PRRSV. After 1 h of viral adsorption, the culture medium was discarded and replaced with fresh DMEM-2% FBS. The cells were incubated for 4 additional days, and GFP fluorescence was observed under a fluorescence microscope (ECLIPSE Ti-S, Nikon, Japan). The Reed–Muench method was used to calculate the $TCID_{50}$.

Protein Expression Analysis by Western Blot

Marc-145 cells were washed three times with PBS and lysed with RIPA buffer (Beyotime, China) on ice for 10 min. Protein concentrations were quantified by BCA protein assay (Beyotime, China). After that, the samples were separated by sodium dodecyl sulfate-polyacrylamide gel electrophoresis (SDS-PAGE) and transferred to polyvinylidene fluoride membranes (PVDF, Millipore, USA). The membranes were blocked with 5% low-fat milk for 2 h at room temperature (RT) and then incubated first with primary antibodies against PRRSV N (1:1000), JNK (1:1000; CST, USA), Phospho-JNK (1:1000; CST, USA), Caspase-3 (1:1000; CST, USA), Cleaved PARP (1:1000; HuaBio, China) on a shaker for 1 h and then incubated with HRP-conjugated goat anti-rabbit IgG or goat anti-rabbit secondary antibodies (1:20,000; Beyotime, China) for 2 h at RT. The membranes were subsequently washed with TBST and detected by the MiniChemi chemiluminescence imaging system (Sage, China). The monoclonal antibody used to detect PRRSV N was produced in our lab. β-actin was detected with an anti-β-actin monoclonal antibody (Bioss, China) to demonstrate equal protein sample loading.

Measurement of Intracellular ROS Level

The reactive oxygen species (ROS) generation was evaluated using a dihydroethidium (DHE) assay kit. Marc-145 cells were seeded in 96-well plates and exposed to different treatments. At the end of the incubation period, the supernatant was discarded. Cells were then stained with 10 μM of DHE (Applygen, China) in the dark at 37°C for 30 min. Subsequently, the cells were washed with PBS three times to remove the unreacted DHE. Then fluorescence intensity was detected by a fluorescence microplate reader (BioTek Synergy H1, Agilent, USA) with an excitation and emission wavelength of 535 and 610 nm.

Flow Cytometry Analysis of Cell Apoptosis

Apoptosis of Marc-145 cells was determined by detecting phosphatidylserine exposure on the cell surface using the fluorescent dye Annexin V-PE apoptosis detection kit (Beyotime, China) according to the manufacturer's protocol. At the end of the treatment period, Marc-145 cells were digested with 0.25% trypsin and washed twice with cold PBS. 5–10×10^4 cells were resuspended in 195 μL binding buffer, then 5 μL Annexin V-PE was added and incubated for 15 min at room temperature in the dark. Finally, cells were analyzed by flow cytometry within 1 h after staining.

Statistical Analysis

All statistical analyses were performed using GraphPad Prism (version 7.0, GraphPad Software, San Diego, CA, USA). One-way ANOVA was used to compare differences between groups. All values in each treatment group are presented as mean ± standard deviation (SD). The threshold for defining statistical significance was set to 0.05 and 0.01.

Results

Characterization of CS-SeNPs

The morphology of SeNPs and CS-SeNPs was analyzed using SEM and TEM. Bare (uncoated) SeNPs were easily aggregated and precipitated, while CS-SeNPs were homogeneous spherical particles with smaller diameters (Figures 1A and B). The

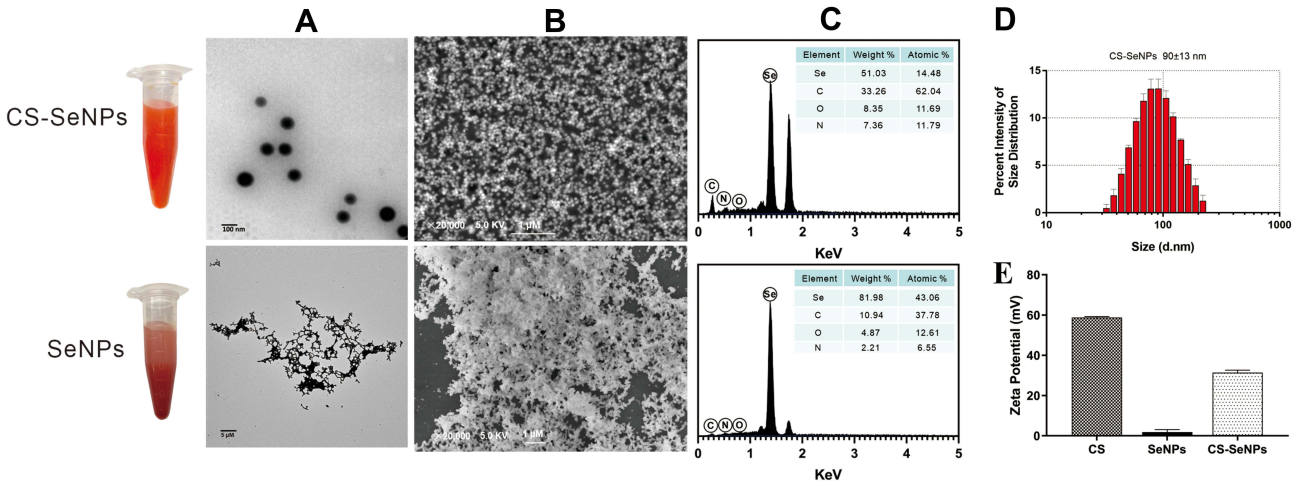

Figure 1 Characterization of CS-SeNPs and SeNPs. The TEM (**A**) and SEM (**B**) micrographs of CS-SeNPs and SeNPs; (**C**) Elemental composition analysis of CS-SeNPs and SeNPs; (**D**) Size distribution of CS-SeNPs by DLS; (**E**) Zeta potentials of CS, SeNPs and CS-SeNPs.

Abbreviations: CS, chitosan; CS-SeNPs, chitosan-coated selenium nanoparticles; DLS, dynamic light scattering; SEM, Scanning electron microscope; TEM, transmission electron microscope.

elemental composition analysis indicated that CS-SeNPs were composed of 51.03% Selenium, 33.26% Carbon, 8.35% Oxygen and 7.36% Nitrogen, and SeNPs consisted of 81.98% Selenium, 10.94% Carbon, 4.87% Oxygen and 2.21% Nitrogen (Figure 1C). The average diameter of CS-SeNPs was 90±13 nm (Figure 1D). The Se concentration in CS-SeNPs was 883.26 mg/L. As an electrokinetic potential, the zeta potential is usually used to evaluate the stability of nanosystems. As shown in Figure 1E, the zeta potential of CS was 58.8±0.37 mV, bare SeNPs was 1.82 ±1.02 mV, and it increased to 31.4 ± 0.99 mV in the presence of CS. The high zeta potential of CS-SeNPs indicated great stability of SeNPs functionalized with CS. CS-SeNPs were highly dispersible in water for over 30 days without any aggregation and precipitation observed. The high stability of CS-SeNPs under physiological conditions highlighted their potential for medical application.

Cell Viability of Marc-145 Cells Treated with CS-SeNPs

The cytotoxic effect of CS-SeNPs on Marc-145 cells was evaluated by the CCK-8 assay. As shown in Figure 2, no significant change in cell viability was observed in Marc-145 cells treated with 0.1, 1, and 10 μM of CS-SeNPs. At

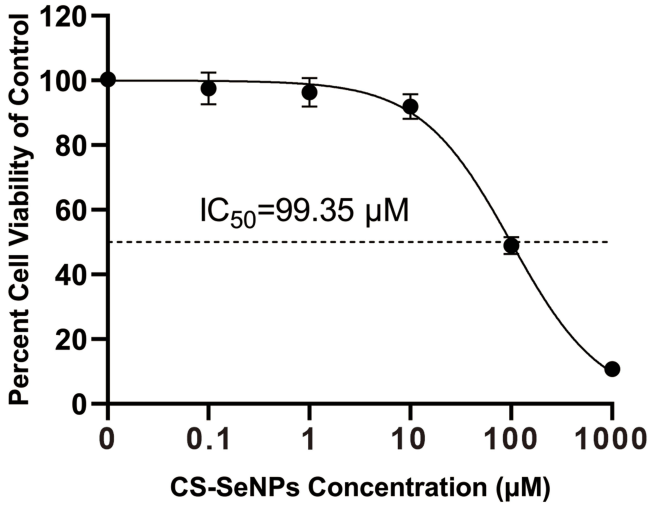

Figure 2 Cell viability of Marc-145 cells treated with different CS-SeNPs concentrations for 48 h using CCK-8 assay. Results are expressed as the mean ± SD of triplicate experiments.

Abbreviations: CS-SeNPs, chitosan-coated selenium nanoparticles; CCK-8, Cell-counting kit 8; IC50, Half-maximal inhibitory concentration; Marc-145, African green monkey kidney epithelial cell line; SD, standard deviation.

concentrations of 100 and 1000 μM, cell viability was significantly lower than the control group. The IC50 of CS-SeNPs for Marc-145 was 99.35 μM. Accordingly, 10 μM CS-SeNPs were used in the following treatments.

CS-SeNPs Alleviated PRRSV-Stimulated Oxidative Stress

Se plays an essential role in oxidation-reduction systems as an essential trace element. We explored whether the inhibitory activity of CS-SeNPs against r-PRRSV-EGFP infection was related to its antioxidant activity. The increase in H_2O_2 initially induced by r-PRRSV-EGFP infection at 48 hours post-infection (hpi) was suppressed by CS-SeNPs (Figure 3A). GSH is well-established as the most important low molecular weight antioxidant synthesized in cells. As shown in Figure 3B, the GSH content was dramatically decreased in r-PRRSV-EGFP infected cells at 48 hpi, and CS-SeNPs treatment restored GSH levels in infected cells. Furthermore, the GSH-Px activity was significantly increased in two CS-SeNPs treatment group cells at 24 and 48 hpi, while no significant changes were observed in r-PRRSV-EGFP infected cells (Figure 3C).

Inhibition of PRRSV Replication in Marc-145 Cells by CS-SeNPs

To validate the effect of CS-SeNPs on PRRSV replication, Marc-145 cells were infected with r-PRRSV-EGFP at 0.1 MOI and treated with CS (1 mg/mL), Na_2SeO_3 (10 μM), and CS-SeNPs (10 μM) respectively for 48 h. At the end of the incubation period, the supernatant was collected and used for RT-qPCR analysis. As shown in Figure 4A, treatment with CS-SeNPs resulted in decreased viral RNA levels ($P<0.01$), while no significant change in r-PRRSV-EGFP replication was observed in CS and Na_2SeO_3 treatment groups ($P>0.05$).

As shown in the timeline schematic, a time-of-addition experiment was performed to investigate the mechanism underlying the inhibitory effect of CS-SeNPs on r-PRRSV-EGFP (Figure 4B). At 48 hpi, culture supernatants were harvested for RNA isolation and qRT-PCR-based analysis. The results showed that PRRSV RNA levels were significantly decreased in the CS-SeNPs treatment groups (groups I, III, V, and VII) compared with the control group. However, no significant change was observed in group IV cells treated with CS-SeNPs for 1 h before PRRSV infection. After Marc-145 cells in groups II and VI were treated with CS-SeNPs and PRRSV for 1 h, PRRSV was suppressed to a lower extent than in the CS-SeNPs treatment groups (Figure 4C). Taken together, these findings indicate that CS-SeNPs do not exert a direct virucidal effect on PRRSV and may inhibit PRRSV during the late stages of viral replication or improve host antiviral ability. Moreover, the treatment used for group VII was adopted in the following experiments.

To further verify the inhibitory effect of CS-SeNPs in PRRSV replication, Marc-145 cells were infected with PRRSV (0.1 MOI, r-PRRSV-EGFP or ZJ-JX/2015) and incubated with 10 μM CS-SeNPs for 48 h. ORF5 mRNA levels were significantly decreased at 24 to 48 hpi, and $TCID_{50}$ assays showed that viral titers significantly decreased at 36 to 48 hpi in CS-SeNPs treated Marc-145 cells (Figures 4D and E). The $TCID_{50}$ assay is a method to quantify virus infectivity in

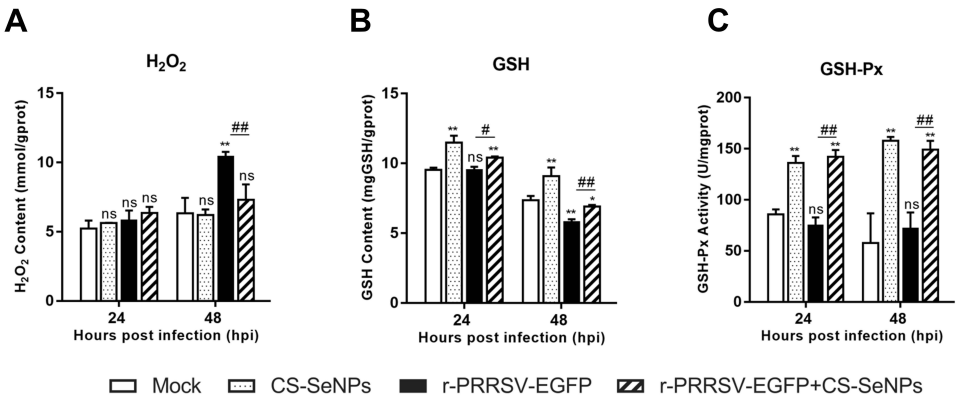

Figure 3 CS-SeNPs suppress oxidative stress induced by r-PRRSV-EGFP in Marc-145 cells. Effects of CS-SeNPs on H_2O_2 (**A**) and GSH (**B**) content and GSH-Px activity (**C**) in r-PRRSV-EGFP infected Marc-145 cells. All results are expressed as the mean ± SD of triplicate experiments. *P<0.05, **P <0.01 compared with mock, #P<0.05, ##P <0.01 compared with r-PRRSV-EGFP infected cells.

Abbreviations: CS-SeNPs, chitosan-coated selenium nanoparticles; GSH, glutathione; GSH-Px, glutathione peroxidase; H_2O_2, hydrogen peroxide; SD, standard deviation.

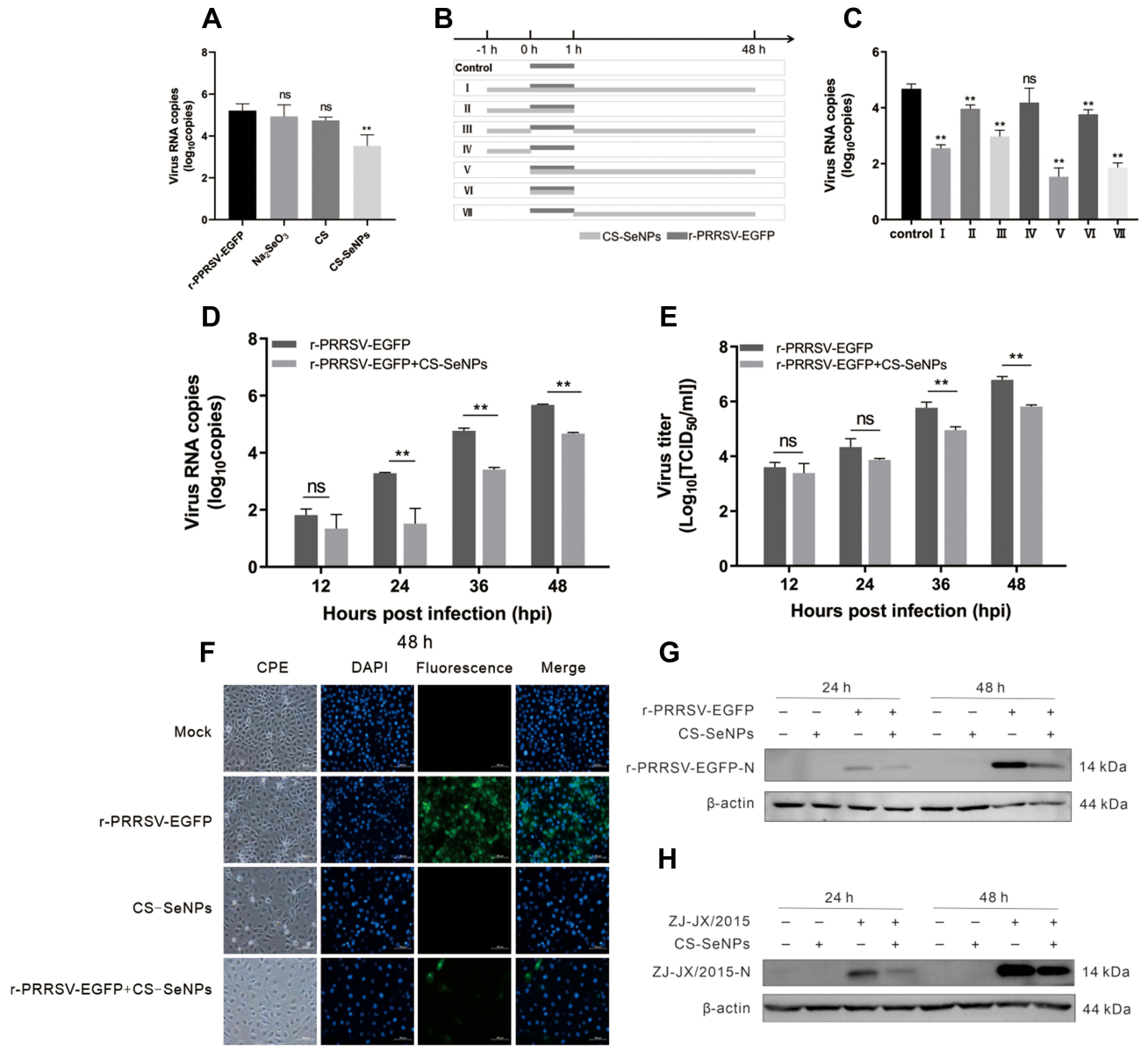

Figure 4 Identification of the inhibitory effect of CS-SeNPs on PRRSV replication in Marc-145 cells. (**A**) Relative r-PRRSV-EGFP ORF 5 mRNA levels determined by qRT-PCR in Marc-145 inoculated with r-PRRSV-EGFP at 0.1 MOI and treated with CS (1 mg/mL), Na_2SeO_3 (10 μM), and CS-SeNPs (10 μM) for 48 h. (**B**) Time-of-addition schematic. (**C**) Relative r-PRRSV-EGFP ORF 5 mRNA levels in Marc-145 inoculated with r-PRRSV-EGFP at 0.1 MOI and treated with CS-SeNPs (10 μM) according to the schematic. **P <0.01 compared with control group cells. (**D**) Relative ORF 5 mRNA levels determined by qRT-PCR. **P <0.01 compared with r-PRRSV-EGFP infected cells. (**E**) Viral titers detected by $TCID_{50}$ of r-PRRSV-EGFP according to group VII treatment pattern in Figure 4B at the indicated times. Results are expressed as the mean ± SD of triplicate experiments, **P <0.01 compared with r-PRRSV-EGFP infected cells. (**F**) Marc-145 cells infected with r-PRRSV-EGFP at an MOI of 0.1 for 1 h and incubated with or without 10 μM CS-SeNPs for 48 h. Cells were fixed and stained with DAPI (4′,6-diamidino-2-phenylindole) and observed under fluorescence microscopy. Western blot analysis of PRRSV N protein in Marc-145 cells infected with r-PRRSV-EGFP (**G**) and ZJ-JX/2015 (**H**) and then incubated with or without 10 μM CS-SeNPs for 24 and 48 h. β-actin was used as the loading control.

Abbreviations: CS, chitosan; CS-SeNPs, chitosan-coated selenium nanoparticles; MOI, multiplicity of infection; ORF5, open reading frame 5; qRT-PCR, Quantitative Real-time Polymerase chain reaction; SD, standard deviation; $TCID_{50}$, the median tissue culture infectious dose.

cells, while RT-qPCR is suitable for rapidly quantifying virus particles in cell supernatant irrespective of viral infectivity. Accordingly, RT-qPCR may be more sensitive than $TCID_{50}$ in determining the quantification of PRRSV particles in cell supernatant. Interestingly, r-PRRSV-EGFP carries an EGFP reporter gene as a separate transcription unit which can be useful to monitor PRRSV spread. As shown in Figure 4F, the fluorescence intensity, used as an indicator of r-PRRSV-EGFP concentrations, was significantly lower in the CS-SeNPs-treated group than in the control group at 48 hpi. Western

blot analysis demonstrated that CS-SeNPs could effectively reduce the replication of r-PRRSV-EGFP and ZJ-JX/2015 strains at 24 and 48 hpi (Figure 4G and H).

CS-SeNPs Inhibit Apoptosis Induced by r-PRRSV-EGFP Through ROS/JNK Signaling in Marc-145 Cells

In Marc-145 cells, PRRSV infection could induce oxidative stress in cells by generating ROS, playing an important role in PRRSV pathogenesis. Current evidence suggests that excess cellular levels of ROS cause damage to proteins, playing an essential role in apoptosis. As expected, the ROS levels were significantly increased in the r-PRRSV-EGFP group at 48 hpi, and CS-SeNPs treatment significantly reduced ROS production induced by r-PRRSV-EGFP in Marc-145 cells (Figure 5A). There is ample evidence that PRRSV could induce apoptosis during the late stages of infection in Marc-145 cells. Accordingly, we evaluated the effect of CS-SeNPs on apoptosis induced by r-PRRSV-EGFP using Annexin V-PE fluorescent dye. For the quantitative assessment of apoptosis, Marc-145 cells were infected with r-PRRSV-EGFP (MOI= 0.1) for 1 h and then incubated with or without 10 μM CS-SeNPs for 48 h. As illustrated in Figures 5B and C, the apoptosis ratio was significantly increased to 34.8 ± 0.6% following infection with r-PRRSV-EGFP, while CS-SeNPs treatment significantly decreased the apoptosis rate (17.2 ± 0.3%). We further analyzed the protein expression level of key molecules, including p-JNK, JNK, caspase-3, cleaved-caspase-3, cleaved-PARP, and PRRSV-N by Western blot. As shown in Figures 5D and E, we found that r-PRRSV-EGFP infection could upregulate the expression of p-JNK, cleaved-

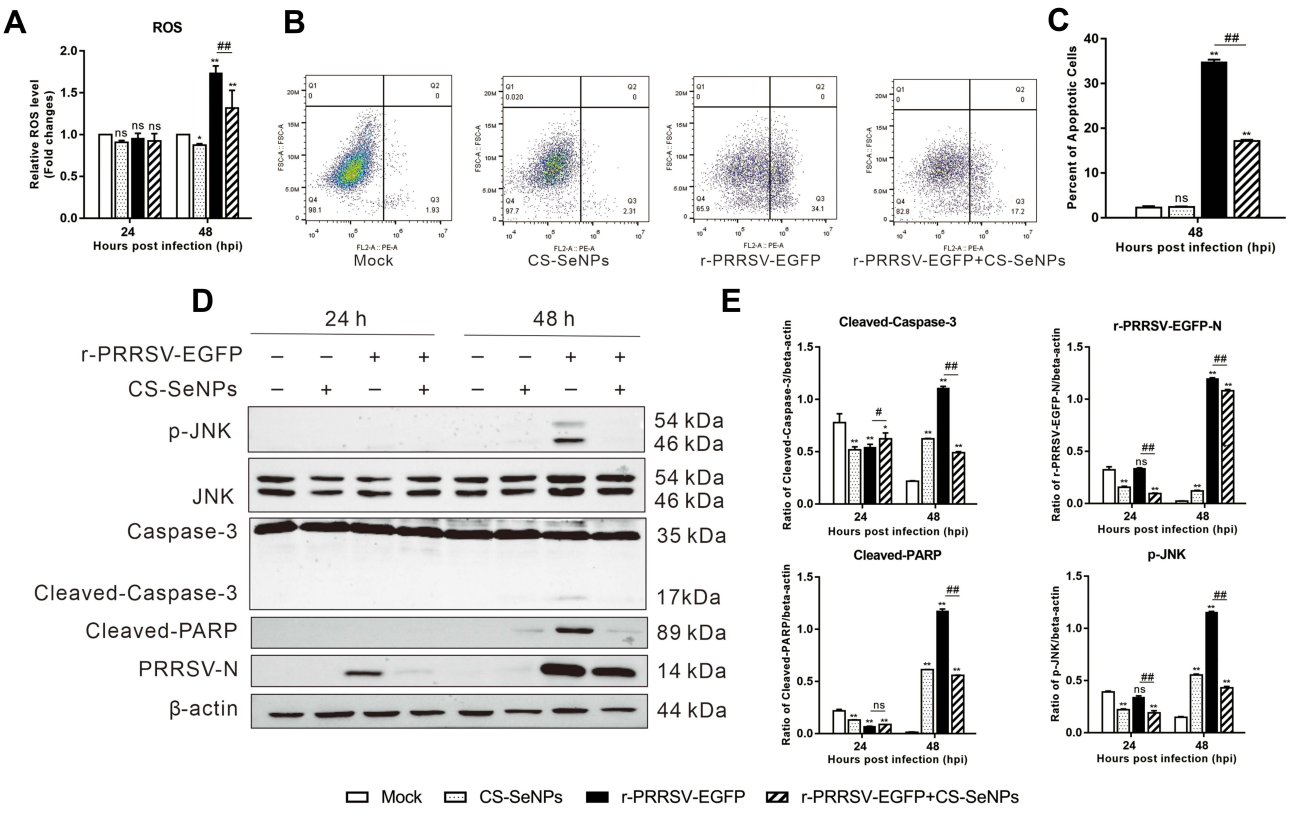

Figure 5 CS-SeNPs inhibit Marc-145 cell apoptosis caused by r-PRRSV-EGFP. Marc-145 cells were infected with r-PRRSV-EGFP (MOI= 0.1) for 1 h and then incubated with or without 10 μM CS-SeNPs for 24 or 48 h. (**A**) ROS levels were detected by DHE fluorescence intensity. (**B**) Flow cytometry analysis of apoptosis rate of Marc-145 cells stained with Annexin V-PE at 48 hpi. (**C**) Quantitative analysis of apoptotic cells expressed as the mean ± SD of triplicate experiments. (**D**) Protein expression of p-JNK, JNK, caspase-3, cleaved-caspase-3, cleaved-PARP, and PRRSV-N in Marc-145 cells were evaluated by Western blot at 24 and 48 hpi. β-actin was used as the loading control. (**E**) Protein expression was quantified by Western blot and expressed as fold change relative to β-actin. All results are represented as the means ± SD of triplicate experiments. *P<0.05, **P <0.01 compared with mock, #P<0.05, ##P <0.01 compared with r-PRRSV-EGFP infected cells.

Abbreviations: CS-SeNPs, chitosan-coated selenium nanoparticles; DHE, dihydroethidium; hpi, hours post infection; MOI, multiplicity of infection; JNK, reactive oxygen species; PARP, poly adenosinediphosphate-ribose polymerase; N, nucleocapsid; ROS; reactive oxygen species; SD, standard deviation.

caspase-3, and cleaved-PARP in Marc-145 cells at 48 hpi. Notably, the protein levels of p-JNK, cleaved-caspase-3, and cleaved-PARP were significantly reduced when Marc-145 cells were treated with CS-SeNPs for 48 h.

Discussion

It is well-established that SeNPs can be synthesized by physical, chemical, and biological methods.[30] A chemical reduction was used to generate SeNPs in this study. As an abundant natural polysaccharide, CS can interact with SeNPs and prevent them from aggregating due to their hydrophilic groups.[26] Herein, we prepared SeNPs via a one-step method by reducing Na_2SeO_3 with ascorbic acid and stabilizing them with CS. The results demonstrated that the synthesized CS-SeNPs were sub-100 nm monodisperse uniformly spherical nanoparticles stable for approximately 30 days in aqueous solutions. It is well recognized that SeNPs exhibit anti-tumor,[31] anti-oxidant,[32] anti-bacterial,[33] anti-fungal,[34] anti-inflammatory,[35] and anti-viral activities.[19] The present study demonstrated that CS-SeNPs could significantly inhibit PRRSV proliferation and PRRSV-induced oxidative stress in Marc-145 cells, providing compelling evidence of their promising therapeutic potential against PRRSV infection.

Changes in redox homeostasis are key events that favor virus replication and contribute to the pathogenesis of viral diseases.[36] Overwhelming evidence substantiates that PRRSV induces oxidative stress in Marc-145 cells, PAMs, and lung tissues of infected pigs.[28] Consistently, we found that r-PRRSV-EGFP increased the production of ROS and H_2O_2 and reduced GSH generation, especially at 48 hpi. As a key ROS, H_2O_2 is produced endogenously primarily in the mitochondria.[37] Given that excess H_2O_2 can trigger apoptosis, H_2O_2 is currently the most widely used apoptosis inducer due to its broad cytotoxic efficacy against nearly all cell types.[38] Interestingly, targeting host cell factors required for viral infection is another therapeutic approach to fighting viral infections.[39] Host-targeted antiviral therapy has emerged as a new strategy to counter viral resistance and develop broad-spectrum antivirals.[9,39] Current evidence suggests that GSH exhibits antiviral activity by different mechanisms of action, including inhibition of the nuclear factor (NF-κB) signaling pathway, hindrance of viral entry, and interference with viral protein synthesis and folding.[40] Moreover, the efficacy of GSH and pro-GSH molecules as viral inhibitors has been established.[40] This study provided compelling evidence that CS-SeNPs treatment could effectively counter the r-PRRSV-EGFP-induced decline in GSH concentration and maintain redox homeostasis. Notably, compared with the control group, the activity of GSH-Px in two CS-SeNPs treatment group cells was significantly increased at 24 and 48 hpi. GSH-Px is an intracellular antioxidant enzyme that converts reduced GSH into glutathione disulfide (GSSG).[41] Se is a cofactor of GSH-Px, and se-cysteine is the active center of GSH-Px; there is a well-documented relationship between Se and GSH-Px activity.[42] The present study results indicated that CS-SeNPs could enter cells and synthesize and utilize GSH-Px. Moreover, GSH-Px activity decreased with no significant changes in PRRSV infected-Marc-145 cells at 24 hpi. The activity of GPX-1, a member of the GSH-Px family, was reduced in H_1N_1 infected MDCK cells, and SeNPs treatment increased GPX-1 activity, consistent to a certain extent with findings reported by Liu et al. In addition to its antioxidant effect, Se plays an important role in immune regulation in the form of selenoprotein.[43] Yao et al reported that Se supplementation could enhance GPX4 expression in T cells, increase follicular helper T cell numbers and promote antibody responses in immunized mice and young adults after influenza vaccination.[44] Nevertheless, the absorption, bio-transformation, and utilization of CS-SeNPs in mammalian cells remain poorly understood, warranting further studies.

Moreover, we found that treatment with CS-SeNPs reduced the RNA levels of r-PRRSV-EGFP, while separate incubation of CS and Na_2SeO_3 resulted in no significant change in r-PRRSV-EGFP replication levels. Furthermore, RNA levels and viral titers of r-PRRSV-EGFP and the N protein expression levels of r-PRRSV-EGFP and ZJ-JX/2015 PRRSV stain were suppressed by CS-SeNPs in Marc-145 cells. Nonetheless, the mechanisms behind these antiviral activities are largely understudied. Indeed, apoptosis is a programmed cell death defined by characteristic morphological, biochemical, and molecular changes.[45] If properly initiated, apoptosis can limit viral infection by killing virus-infected cells. In response to these stimuli, many viruses have co-evolved to hijack or manipulate these processes to escape host immunity.[46] Moreover, during the eclipse phase of viral infection, when replication and synthesis of viral proteins are at their peak, PRRSV can block cellular antiviral defense mechanisms and hijack host apoptosis for dissemination and infection. Growing evidence corroborates that PRRSV can suppress host apoptosis at an early stage of infection by activating the PI3K/AKT pathway[47,48] and inhibiting the pro-apoptotic protein Bad.[49] This study found ROS production

in Marc-145 cells infected with r-PRRSV-EGFP was significantly altered at 48 hpi, but not at 24 hpi, compared with control group cells. Besides, the apoptosis rates were significantly increased in response to r-PRRSV-EGFP stimulation at 48 hpi. Furthermore, CS-SeNPs treatment significantly reduced ROS production and apoptosis rate induced by r-PRRSV-EGFP in Marc-145 cells. Previous studies have shown that ROS generation is a critical mediator in PRRSV-induced activation of the JNK signaling pathway and apoptosis in Marc-145 cells.[50] Importantly, our data demonstrated that the JNK pathway was activated in r-PRRSV-EGFP infected Marc-145 cells at 48 hpi, leading to significantly increased JNK phosphorylation and cleaved-caspase 3 and cleaved PARP protein expression levels. Activated caspase-3 cleaves proteins, including poly (ADP-ribose) polymerase-1 (PARP-1), have been established to be important in DNA repair and promoting apoptosis.[51] In addition, these changes were significantly inhibited by CS-SeNPs treatment. These results indicated that CS-SeNPs could attenuate PRRSV-induced apoptosis by ROS/JNK-mediated signaling. Consistently, Liu et al reported that SeNPs could inhibit H_1N_1 influenza virus-induced apoptosis by ROS-mediated signaling pathways.[43]

Conclusion

In conclusion, the present study demonstrated that CS-SeNPs synthesized by chemical reduction could enhance antioxidant capacity and effectively suppress PRRSV-induced apoptosis in Marc-145 cells via the ROS/JNK signaling pathway, thereby inhibiting PRRSV replication. This is the first report of the antiviral effect of CS-SeNPs against PRRSV infection, providing the foothold for further studies to develop novel therapeutic approaches.

Acknowledgments

Special thanks to Dr. Chengbao Wang (Northwest A&F University) for providing rHP-PRRSV/SD16/TRS6-EGFP strain in this study. This study was supported by the following grants: Zhejiang Provincial Natural Science Foundation (No. LY22C180003, LQ20C180002, LQ19C180003 and 2021SNLF023); the National Natural Science Foundation of China (No. 31802258, 31802207, 31972656 and 31902249); the Talent Startup Project of Zhejiang Agriculture and Forestry University Scientific Research Development Fund (No. 2022FR008, 2020FR045, 2018FR009 and 2019FR013); Department of Education of Zhejiang Province (No. Y202044917); Key Research and Development Program of Zhejiang Province (2019C02043).

Disclosure

The authors declare no competing financial interests and no conflicts of interest for this work.

References

1. Rossow KD. Porcine reproductive and respiratory syndrome. *Vet Pathol*. 1998;35(1):1–20.
2. Albina E. Epidemiology of porcine reproductive and respiratory syndrome (PRRS): an overview. *Vet Microbiol*. 1997;55(1–4):309–316.
3. Meulenberg JJ. PRRSV, the virus. *Vet Res*. 2000;31(1):11–21.
4. Malgarin CM, Moser F, Pasternak JA, et al. Fetal hypoxia and apoptosis following maternal porcine reproductive and respiratory syndrome virus (PRRSV) infection. *BMC Vet Res*. 2021;17(1):182.
5. Chen X, Zhang Q, Bai J, et al. The Nucleocapsid Protein and Nonstructural Protein 10 of Highly Pathogenic Porcine Reproductive and Respiratory Syndrome Virus Enhance CD83 Production via NF-kappaB and Sp1 Signaling Pathways. *J Virol*. 2017;91(18):e00986–17.
6. Zhao K, Ye C, Chang XB, et al. Importation and Recombination Are Responsible for the Latest Emergence of Highly Pathogenic Porcine Reproductive and Respiratory Syndrome Virus in China. *J Virol*. 2015;89(20):10712–10716.
7. Lunney JK, Fang Y, Ladinig A, et al. Porcine Reproductive and Respiratory Syndrome Virus (PRRSV): pathogenesis and Interaction with the Immune System. *Annu Rev Anim Biosci*. 2016;4:129–154.
8. Guo Z, Chen XX, Li R, et al. The prevalent status and genetic diversity of porcine reproductive and respiratory syndrome virus in China: a molecular epidemiological perspective. *Virol J*. 2018;15(1):2.
9. Kaufmann SHE, Dorhoi A, Hotchkiss RS, et al. Host-directed therapies for bacterial and viral infections. *Nat Rev Drug Discov*. 2018;17(1):35–56.
10. An TQ, Li JN, Su CM, et al. Molecular and Cellular Mechanisms for PRRSV Pathogenesis and Host Response to Infection. *Virus Res*. 2020;286:197980.
11. Lee C. Therapeutic Modulation of Virus-Induced Oxidative Stress via the Nrf2-Dependent Antioxidative Pathway. *Oxid Med Cell Longev*. 2018;2018:6208067.
12. Roman M, Jitaru P, Barbante C. Selenium biochemistry and its role for human health. *Metallomics*. 2014;6(1):25–54.
13. Broome CS, McArdle F, Kyle JA, et al. An increase in selenium intake improves immune function and poliovirus handling in adults with marginal selenium status. *Am J Clin Nutr*. 2004;80(1):154–162.
14. Nunnari G, Coco C, Pinzone MR, et al. The role of micronutrients in the diet of HIV-1-infected individuals. *Front Biosci*. 2012;4(7):2442–2456.
15. Steinbrenner H, Al-Quraishy S, Dkhil MA, et al. Dietary selenium in adjuvant therapy of viral and bacterial infections. *Adv Nutr*. 2015;6(1):73–82.

16. Hiffler L, Rakotoambinina B. Selenium and RNA Virus Interactions: potential Implications for SARS-CoV-2 Infection (COVID-19). *Front Nutr*. 2020;7:164.
17. Hosnedlova B, Kepinska M, Skalickova S, et al. Nano-selenium and its nanomedicine applications: a critical review. *Int J Nanomedicine*. 2018;13:2107–2128.
18. Huang YY, Su EZ, Ren JS, et al. The recent biological applications of selenium-based nanomaterials. *Nano Today*. 2021;38:101205.
19. Wang C, Chen H, Chen D, et al. The Inhibition of H1N1 Influenza Virus-Induced Apoptosis by Surface Decoration of Selenium Nanoparticles with beta-Thujaplicin through Reactive Oxygen Species-Mediated AKT and p53 Signaling Pathways. *ACS Omega*. 2020;5(47):30633–30642.
20. Li Y, Lin Z, Guo M, et al. Inhibition of H1N1 influenza virus-induced apoptosis by functionalized selenium nanoparticles with amantadine through ROS-mediated AKT signaling pathways. *Int J Nanomedicine*. 2018;13:2005–2016.
21. Zhong JY, Xia Y, Hua L, et al. Functionalized selenium nanoparticles enhance the anti-EV71 activity of oseltamivir in human astrocytoma cell model. *Artif Cells Nanomed Biotechnol*. 2019;47(1):3485–3491.
22. Mahdavi M, Mavandadnejad F, Yazdi MH, et al. Oral administration of synthetic selenium nanoparticles induced robust Th1 cytokine pattern after HBs antigen vaccination in mouse model. *J Infect Public Health*. 2017;10(1):102–109.
23. Elieh-Ali-Komi D, Hamblin MR. Chitin and Chitosan: production and Application of Versatile Biomedical Nanomaterials. *Int J Adv Res*. 2016;4 (3):411–427.
24. Dorazilova J, Muchova J, Smerkova K, et al. Synergistic Effect of Chitosan and Selenium Nanoparticles on Biodegradation and Antibacterial Properties of Collagenous Scaffolds Designed for Infected Burn Wounds. *Nanomaterials*. 2020;10(10):1971.
25. Wang C, Huang B, Kong N, et al. A novel porcine reproductive and respiratory syndrome virus vector system that stably expresses enhanced green fluorescent protein as a separate transcription unit. *Vet Res*. 2013;44:104.
26. Zeng S, Ke Y, Liu Y, et al. Synthesis and antidiabetic properties of chitosan-stabilized selenium nanoparticles. *Colloids Surf B Biointerfaces*. 2018;170:115–121.
27. Awet TT, Kohl Y, Meier F, et al. Effects of polystyrene nanoparticles on the microbiota and functional diversity of enzymes in soil. *Environ Sci Eur*. 2018;30(1):11.
28. Liu X, Song Z, Bai J, et al. Xanthohumol inhibits PRRSV proliferation and alleviates oxidative stress induced by PRRSV via the Nrf2-HMOX1 axis. *Vet Res*. 2019;50(1):61.
29. Ding Y, Li G, Cheng F, et al. Yansuanmalingua inhibits replication of type 2 porcine reproductive and respiratory syndrome virus via activating the caspase-8 apoptosis pathway. *J Basic Microbiol*. 2020;60(5):400–406.
30. Johnson J, Shanmugam R, Lakshmi T. A review on plant-mediated selenium nanoparticles and its applications. *J Popul Ther Clin Pharmacol*. 2022;28(2):e29–e40.
31. Rajkumar K, Sandhya MVS, Koganti S, et al. Selenium Nanoparticles Synthesized Using Pseudomonas stutzeri (MH191156) Show Antiproliferative and Anti-angiogenic Activity Against Cervical Cancer Cells. *Int J Nanomed*. 2020;15:4523–4540.
32. Mehanna ET, Khalaf SS, Mesbah NM, et al. Anti-oxidant, anti-apoptotic, and mitochondrial regulatory effects of selenium nanoparticles against vancomycin induced nephrotoxicity in experimental rats. *Life Sci*. 2022;288:120098.
33. Hernandez-Diaz JA, Garza-Garcia JJ, Leon-Morales JM, et al. Antibacterial Activity of Biosynthesized Selenium Nanoparticles Using Extracts of Calendula officinalis against Potentially Clinical Bacterial Strains. *Molecules*. 2021;26(19):5929.
34. Shakibaie M, Salari Mohazab N, Ayatollahi Mousavi SA. Antifungal Activity of Selenium Nanoparticles Synthesized by Bacillus species Msh-1 Against Aspergillus fumigatus and Candida albicans. *Jundishapur J Microbiol*. 2015;8(9):e26381.
35. El-Ghazaly MA, Fadel N, Rashed E, et al. Anti-inflammatory effect of selenium nanoparticles on the inflammation induced in irradiated rats. *Can J Physiol Pharmacol*. 2017;95(2):101–110.
36. Fraternale A, Zara C, De Angelis M, et al. Intracellular Redox-Modulated Pathways as Targets for Effective Approaches in the Treatment of Viral Infection. *Int J Mol Sci*. 2021;22(7):3603.
37. Basu S, Rajakaruna S, Dickinson BC, et al. Endogenous hydrogen peroxide production in the epithelium of the developing embryonic lens. *Mol Vis*. 2014;20:458–467.
38. Xiang J, Wan C, Guo R, et al. Is Hydrogen Peroxide a Suitable Apoptosis Inducer for All Cell Types? *Biomed Res Int*. 2016;2016:7343965.
39. Bekerman E, Einav S. Infectious disease. Combating emerging viral threats. *Science*. 2015;348(6232):282–283.
40. Fraternale A, Paoletti MF, Casabianca A, et al. GSH and analogs in antiviral therapy. *Mol Aspects Med*. 2009;30(1–2):99–110.
41. Lubos E, Loscalzo J, Handy DE. Glutathione peroxidase-1 in health and disease: from molecular mechanisms to therapeutic opportunities. *Antioxid Redox Signal*. 2011;15(7):1957–1997.
42. Batcioglu K, Ozturk C, Karagozler A, et al. Comparison of the selenium level with GSH-Px activity in the liver of mice treated with 7,12 DMBA. *Cell Biochem Funct*. 2002;20(2):115–118.
43. Liu X, Chen D, Su J, et al. Selenium nanoparticles inhibited H1N1 influenza virus-induced apoptosis by ROS-mediated signaling pathways. *RSC Adv*. 2022;12:3862–3870.
44. Yao Y, Chen Z, Zhang H, et al. Selenium-GPX4 axis protects follicular helper T cells from ferroptosis. *Nat Immunol*. 2021;22(9):1127–1139.
45. Gorczyca W, Melamed MR, Darzynkiewicz Z. [Programmed death of cells (apoptosis)]. *Patol Pol*. 1993;44(3):113–119.
46. Pujhari S, Rasgon JL, Zakhartchouk AN. Anti-apoptosis in porcine respiratory and reproductive syndrome virus. *Virulence*. 2016;7(5):610–611.
47. Pujhari S, Baig TT, Zakhartchouk AN. Potential role of porcine reproductive and respiratory syndrome virus structural protein GP2 in apoptosis inhibition. *Biomed Res Int*. 2014;2014:160505.
48. Wang R, Wang X, Wu JQ, et al. Efficient porcine reproductive and respiratory syndrome virus entry in MARC-145 cells requires EGFR-PI3K-AKT -LIMK1-COFILIN signaling pathway. *Virus Res*. 2016;225:23–32.
49. Zhu L, Yang S, Tong W, et al. Control of the PI3K/Akt pathway by porcine reproductive and respiratory syndrome virus. *Arch Virol*. 2013;158 (6):1227–1234.
50. Yin S, Huo Y, Dong Y, et al. Activation of c-Jun NH(2)-terminal kinase is required for porcine reproductive and respiratory syndrome virus-induced apoptosis but not for virus replication. *Virus Res*. 2012;166(1–2):103–108.
51. Sairanen T, Szepesi R, Karjalainen-Lindsberg ML, et al. Neuronal caspase-3 and PARP-1 correlate differentially with apoptosis and necrosis in ischemic human stroke. *Acta Neuropathol*. 2009;118(4):541–552.